ARTICLE

Carbon nanohorn modified platinum electrodes for improved immobilisation of enzyme in the design of glutamate biosensors

Rochelle Ford,[a] Stephen. J. Devereux,[a] Susan. J. Quinn[a]* and Robert. D. O'Neill[a]*

Electrochemical enzymatic biosensors are the subject of research due to their potential for *in vivo* monitoring of glutamate, which is a key neurotransmitter whose concentration is related to healthy brain function. This study reports the use of biocompatible oxidised carbon nanohorns (o-CNH) with a high surface area, to enhance the immobilization of glutamate oxidase (GluOx) for improved biosensor performance. Two families of biosensors were designed to interact with the anionic GluOx. Family-1 consists of covalently functionalised o-CNH possessing hydrazide (HYZ) and amine (PEG–NH$_2$) terminated surfaces and Family-2 comprised non-covalently functionalised o-CNH with different loadings of polyethyleneimine (PEI) to form a cationic hybrid. Amperometric detection of H$_2$O$_2$ formed by enzymatic oxidation of glutamate revealed a good performance from all designs with the most improved performance by the PEI hybrid systems. The best response was from a o-CNH:PEI ratio of 1:10 mg mL^{-1}, which yielded a glutamate calibration plateau, J_{MAX}, of 55 ± 9 μA cm^{-2} and sensitivity of 111 ± 34 μA mM^{-1} cm^{-2}. The low K_M of 0.31 ± 0.05 mM indicated that the retention of the enzyme with a limit of detection of 0.02 ± 0.004 μM and a response time of 0.88 ± 0.13 s. The results demonstrate the high sensitivity of these biosensors and their potential for future use for the detection of glutamate *in-vivo*.

Introduction

Glutamate is the most abundant free amino acid in the brain and the primary excitatory neurotransmitter. The overactivation of glutamate receptors, which are located on the surface of brain cells, can lead to cell death due to excitotoxicity.[1] Therefore, determining glutamate levels in the brain extracellular fluid (ECF) is necessary to understand its role maintaining healthy brain function.[2,3] The common reference method employed to measure glutamate concentration is microdialysis.[4,5] However, this method has low temporal resolution, and the large probe size ~200–500 μm[4] can damage brain tissue and lead to inaccurate determination of glutamate levels.[6] In contrast electrochemical enzyme-based biosensors are less invasive, due to the relatively small probe size, and offer the possibility for miniaturization to yield high temporal and spatial resolution.[7-9]

In addition to the factors above, the key parameters that must be optimised for an effective biosensor are the stability, sensitivity and specificity. To date, we have successfully, prepared glutamate biosensors using L-glutamate oxidase (GluOx), which allows for the detection of glutamate through the oxidation of the sensing by-product H$_2$O$_2$, see Figure 1a. The fabrication of these sensors has involved the use of a Pt electrode due to its high sensitivity to H$_2$O$_2$ and the use of a

blocking polymer to limit the interference of ascorbic acid (AA), which is present in the ECF at significantly higher concentrations (500 μM) compared to Glutamate (10 μM).[10] For example, the use of poly-ortho-phenylenediamine (PoPD) can block AA interference up to 99.8%, while still allowing efficient surface oxidation of H$_2$O$_2$.[11] In addition, the stability of the biosensor was improved by using the cationic polymer polyethyleneimine (PEI) for electrostatic neutralization of the anionic GluOx enzyme layer together with poly-ethylene glycol diglycidyl ether (PEGDE),[12] which is an epoxide polymer that acts as a crosslinker by reacting with the enzyme's amino and carboxyl groups. The reaction of this non-toxic polymer under mild conditions has been shown to retain the enzyme's selectivity to the substrate in the presence of secondary analytes.[13,14] Our previous biosensors have shown high stability (up to 90 days) and high sensitivity to Glutamate (limit of detection <0.2 μM).[12]

The use of nanomaterials to improve biosensor performance is increasingly a subject of interest due to (a) their large surface area, which can be exploited to increase the amount of immobilized enzyme and (b) the potential to offer enhanced electrochemical reactivity of biomolecular analyte.[15] Carbon has proved an electrode material of choice for many years and the use of emergent carbon nanomaterials is providing access to a new generation of sensors with improved capabilities due to enhanced electron transfer, and ready adsorption of molecules.[16-18] To date, carbon nanomaterial immobilised enzyme based biosensors have been reported for the detection of glucose and glutamate using carbon black nanoparticles,[19-21] carbon nanotubes[22,23] carbon nanofibers[24,25] and graphene.[26-29]

[a.] School of Chemistry, University College Dublin, Belfield, Dublin 4, Ireland.
susan.quinn@ucd.ie, robert.oneill@ucd.ie
† Footnotes relating to the title and/or authors should appear here.

Another emergent carbon nanomaterial are carbon nanohorns (CNH), which comprise spherical aggregates, approximately 100 nm in diameter, of sp^2 end capped tubules, see Figure 1b.[30,31] Their unique structure, metal free synthesis combined with low toxicity[31,32] and ease of functionalisation has made them attractive for a range of applications.[33] Notably, the presence of hydrophobic and polar groups at the surface of CNHs are speculated to contribute to their affinity for biological molecules such as peptides.[34] The properties of CNHs have also led them to be considered as an electrochemical biosensing platform. The encapsulation of glucose oxidase in a Nafion-CNHs composite to prepare a biosensor with high sensitivity (1.06 μA/mM) and stability has been reported by *Liu et al*.[35] This sensor combined the high surface area of the CNHs with the ability of Nafion to block the detection of interferant species. Another study by the *Liu* group used CNHs non-covalently modified with a poly(sodium 4-styrenesulfonate) to immobilise the myoglobin enzyme for the effective detection of H_2O_2.[36] Significantly, COOH surface functionalised CNHs have also been shown to possess intrinsic peroxidase-like activity, which has been exploited for the detection of glucose.[37]

Herein we report on the use of surface functionalised CNHs to increase the surface immobilisation of glutamate oxidase (GluOx) for glutamate sensing, which is monitored by the detection of H_2O_2, see Figure 1b. To achieve this CNHs were functionalised to yield favourable electrostatic interactions with the anionic GluOx and its anionic substrate L-glutamate. **Family-1** comprised CNHs covalently functionalised with either (i) a hydrazide group via a short alkyl chain (**CNH-HYZ**) or (ii) a polymer pegylated amine (**CNH-PEG-NH₂**); while **Family-2** consisted of **o-CNH** non-covalently coated with a cationic polyethylene imine polymer (**CNH-PEI**), see Figure 1c. Biosensors were assembled at a Pt electrode surface using

these CNHs, GluOx the PEGDE crosslinking agent. The amperometric response of these materials to the presence of L glutamate was used to investigate performance of the different formulations.

Experimental

2.1 Materials

The SWCNHs were provided by Carbonium Srl (info@carbonium.it, Padova, Italy). Phosphate buffered saline (PBS) tablets, hydrogen peroxide (3% w/w. solution), poly (ethylene) glycol diglycidyl ether (PEGDE) Mn = 500, poly (ethylene) imine (PEI, 50% w/v aqueous solution, ~750 kDa), N-(3-Dimethylaminopropyl)-N-ethylcarbodiimide hydrochloride (EDC), adipic acid dihyrazide, N-hydroxysuccinimide (NHS), and poly(ethylene glycol) bis(amine) 1500 were supplied by Sigma. GluOx (400 U mL^{-1}, recombinant type, Streptomyces sp. X-119-6; EC 1.4.3.11) in phosphate buffered saline (PBS) solution supplied by Enzyme–Sensor Co. Ltd. (Tsukuba, Japan) was stored at −21 °C. PBS stock solutions (pH 7.4) were prepared in Milli-Q® water (18.2 MΩ cm), and stored at 4 °C. A 1% w/v PEI solution was prepared by diluting the PEI solution in H_2O. A 0.3% wt. solution of H_2O_2 was prepared in deionized water and stored at 4 °C.

2.2 Preparation of Oxidised Carbon Nanohorns (o-CNH)

Oxidized CNHs (o-CNH) were prepared by previously reported methods.[39-41] Briefly, 50 mg of pristine CNHs were oxidized in 50 mL of 5 M nitric acid solution for 2 h under reflux at 120 °C. Subsequent washing and centrifugation of the particles afforded aqueous dispersions of o-CNH at a concentration of 2 mg mL^{-1}.
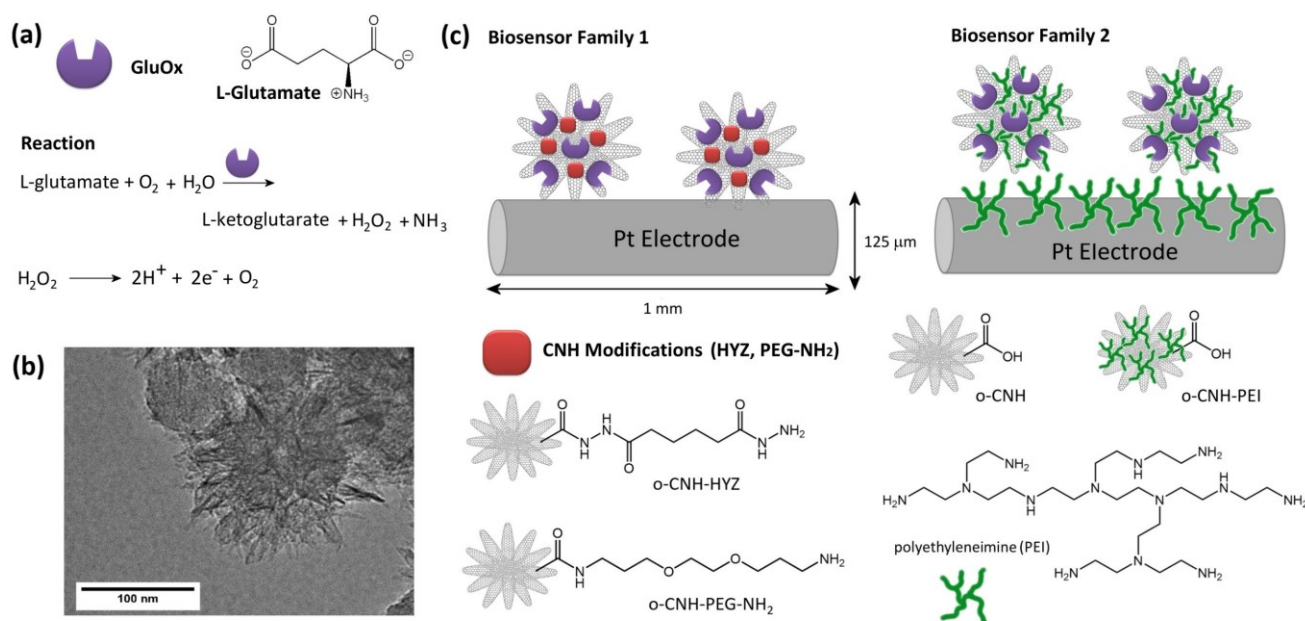

Fig. 1 (a) Oxidation of glutamate by GluOx to yield H_2O_2. (b) TEM image of CNHs. (c) Schematic representation of the designs for the two biosensor families studied.

2.3 Preparation of CNH-PEG-NH₂

1-Ethyl-3-(3-dimethylaminopropyl)-carbodiimide (EDC, 0.25 mol L^{-1}, 1 mL) and N-hydroxysuccinimide (NHS, 0.25 mol L^{-1}, 1 mL) were added to a suspension of **o-CNH** (0.22 mg m L^{-1}, 12 mL). The solution was stirred for 2 h at 20 °C. Bis(2-aminoethyl) polyethylene glycol (0.02 mol L^{-1}, 1 mL) was added to the activated ester CNHs (0.22 mg mL^{-1}, 12 mL) and left to stir at RT overnight. Excess PEG 1500 was washed from the reaction six times with water by centrifugation at 13000 rpm. **CNH-PEG-NH₂** were then dispersed in 5 mL of H₂O. This reaction was repeated twice.

2.4 Preparation of CNH-Hydrazide (CNH-HYZ)

EDC (0.25 mol L^{-1}, 1 mL) and NHS (0.25 mol L^{-1}, 1 mL) were added to a suspension of o-CNHs (0.34 mg mL^{-1}, 10 mL). The solution was stirred for 2 h at 20 °C. Adipic acid dihydrazide (0.17 mol L^{-1}, 1 mL) was added to the activated ester CNHs (0.34 mg mL^{-1}, 10 mL) and left to stir overnight. Excess adipic acid dihydrazide was washed from the reaction six times with water by centrifugation at 13000 rpm. CNHs-HYZ were then dispersed in 5 mL of H₂O. This reaction was repeated twice.

2.5 Preparation of o-CNH/PEI Hybrid Samples

Different volumes of polyethyleneimine 50 % w/v aqueous solution was added to aqueous dispersion of **o-CNH** to prepare dispersions with composition **o-CNH** (0.1 mg mL^{-1}, 1 mg mL^{-1}, 5 mg mL^{-1} and 10 mg mL^{-1}) and PEI (0.1 mg mL^{-1} to 10 mg mL^{-1}). The hybrid samples were typically prepared on the 2 mL scale.

2.6 Characterization

Dynamic light scattering (DLS) and ζ-potential measurements were carried out on a Malvern Zetasizer Nano-ZS, equipped with a 4 mW He-Ne laser operating at 632.8 nm, measurements were taken at 173°. SEM Samples were mounted on stubs using double-sided carbon tape. SEM samples were examined using a FEI Quanta3D FEG Dual Beam (FEI Ltd, Hillsboro, USA).

2.7 Software

Chart™ (ver. 5.2; AD Instruments Ltd., Oxford, UK) software was used for data acquisition and enabled an applied potential of +500 mV vs. a Ag pseudo-reference electrode to be applied. This potential was used for all calibrations. Chart was also required for use of the powerlab interface which was ran using the ACM – IV potentiostat. Prism (ver. 5.01; GraphPad Software, San Diego, CA, USA) was used for data analysis and plotting.

2.8 Electrode preparation and modification

Electrodes were prepared by adapting the method described previously for the preparation of GluOx biosensors in the absence of CNHs.[12,37,38] Briefly, ~2 mm of Teflon® was removed from the Pt-Ir wire to expose the electrode material on both ends of the wire, and was cut more accurately to 1 mm. One end of the wire was soldered to a gold clip. The electrodes were allowed to settle under an applied potential of +0.5 V for 1 h prior to modification. The electrode modification has also been described previously;[12] PEI, GluOx and CNH solutions were immobilized on the biosensor surface by dipping the electrode into the solution for 1 s. CNH solutions were sonicated for 30 min before each deposition onto the electrode surface and the solutions were also sonicated between each dip (~5 min). All electrodes were crosslinked with PEGDE, the modified electrode was inserted into the PEGDE solution (1%) for 5 s, allowed to dry for 5 min and then rinsed in water for 10 min, results are reported for the day of fabrication (day-0), unless otherwise stated.

2.9 Biosensor nomenclature

The nomenclature used to describe the biosensors prepared is briefly as follows: **Pt/GluOx₅** represents the simplest design containing 5 dips of the enzyme GluOx on the Pt electrode, whereas the sequential deposition of a modifier on the surface can be seen in the design **Pt/CNH-PEG₅/GluOx₅**, where 5 dips of CNH-PEG-NH₂ were deposited on the electrode followed by 5 dips of GluOx₅.

2.10 The Electrochemical Cell

All calibrations were carried out in a 20 mL glass cell containing PBS (pH 7.4) at room temperature (21 ± 1 °C). A standard three-electrode set-up was used here which included a reference electrode in the form of a silver pseudo-reference electrode (250 μm diameter Ag wire) and the auxiliary electrode was a stainless-steel needle (0.8 mm diameter). The working electrodes were composed of Pt-Ir wire (90-10 ratio, Advent Research Materials Ltd., Oxford) which were coated in a Teflon® layer (125 μm internal diameter). The response of the biosensors to additions of H₂O₂ and glutamate were recorded in the electrochemical cell. Glutamate injections of 0.05, 0.1 0.2, 0.3, 0.5, 0.7, 1, 2 and 3 mM into PBS solution. The solution was initially allowed to achieve a steady baseline current; the solution was then stirred gently, and an initial aliquot of glutamate was added, stirring was continued until the solution was homogenous, approximately 20 sec, the stirrer was then stopped. Solutions were allowed to become quiescent and the current measurement taken for analysis. This process was repeated for each aliquot of glutamate and similarly for H₂O₂. Representative data of the current response with time is given in Figure S1.

2.11 Hill equation

Michaelis-Menten (Eqn. 1) is typically the most suitable enzyme model used when GluOx is the enzyme being investigated, as the response is typically hyperbolic. This occurs when there is single substrate binding site on the enzyme or if there are many binding sites present but they do not interact cooperatively. However, analysis of the data revealed the use of the Hill equation (Eqn. 2), a variation of Michaelis-Menten, to be more appropriate here in describing the behaviour of GluOx in

complex layers. It was therefore used to obtain the enzyme-kinetic parameters J_{MAX} (an index of enzyme loading between different designs) and the enzyme–substrate affinity term, K_M.[42]

$$J_S = \frac{J_{MAX}}{1 + K_M/[S]} \qquad (1)$$

$$J_S = \frac{J_{MAX}}{1 + (K_M/[S])^h} \qquad (2)$$

2.12 Statistical analysis

Results are reported as the mean ± standard error, where *n* is the number of electrodes. Student t-tests were used to determine the statistical significance of findings between sets; a p < 0.05 using a 95% confidence interval, was deemed to be statistically significant. For DLS and zeta potential measurements results were reported as mean ± standard deviation (SD), where an average of triplicates for each result is reported.

Results and Discussion

Selective glutamate detection requires maintaining the substrate specificity of the enzyme upon immobilization and limiting the detection of interference species. Our most successful biosensor to date featured the enzyme GluOx as the 'sensing element', the cationic polymer PEI to facilitate electrostatic neutralization, and the crosslinker PEGDE for long-term stability of up to three months. This design required two dips of the PEI with five subsequent dips of enzyme (**Pt/PEI₂/GluOx₅**).[12] This formulation was used as a platform to examine the ability CNHs of high surface area, functionalised with amine groups to further enhance the electrode performance by facilitating an increase in GluOx loading through electrostatic interactions with the GluOx lysine groups.

3.1 Preparation and characterization of carbon nanohorn supports

Family-1 systems were prepared by reacting the isolated **o-CNH** with (i) adipic acid dihyrazide and (ii) poly(ethylene glycol) bis(amine) MW 1500, in aqueous solution using standard bioconjugate coupling. This yielded nanohorn samples with a terminal amine group (**CNH-PEG-NH₂**), and a short-chain hydrazide (**CNH-HYZ**), see Figure 1c. Following this reaction, the CNH systems were rigorously washed by repeated centrifugation against water.

DLS measurements of **o-CNH**, **CNH-HYZ** and **CNH-PEG-NH₂** indicated the presence of discrete nanoparticles with no evidence of significant aggregation, see Figure 2a. The average hydrodynamic size of the CNH samples was found to increase
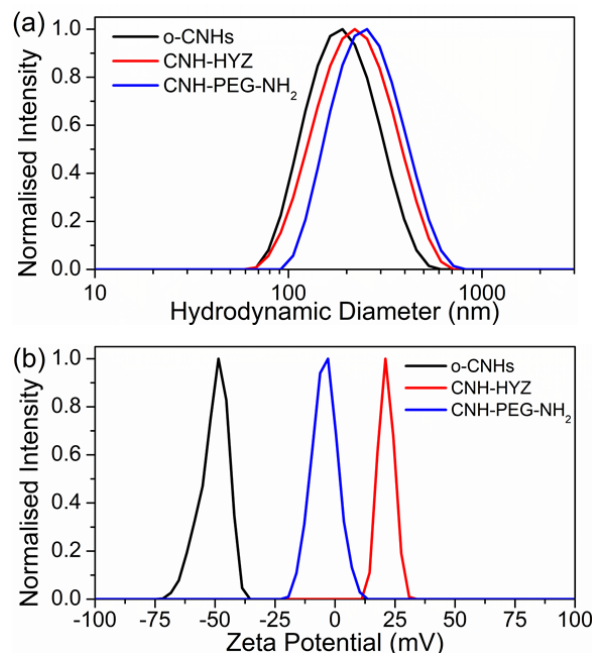

Fig. 2 (a) Dynamic light scattering (b) Zeta potential measurements of **o-CNH, CNH-HYZ** and **CNH-PEG-NH₂** obtained in ddH₂O, pH 7.2 at 25 °C

with surface functionalisation with recorded values of 188 ± 80 (**o-CNHs**), 219 ± 98 (**CNH-HYZ**) and 259 ± 107 nm (**CNH-PEG-NH₂**) for the polymer functionalisation. The large distribution in the hydrodynamic diameter of these particles reflects the different size populations present after oxidation and the presence of some colloidally stable clusters of CNHs. Aqueous dispersions of carboxylic acid functionalised CNHs have shown broad size distributions, ranging from 105-200 nm.[43,44] While the hydrodynamic diameter found in the current study for the modified CNHs are somewhat similar to those reported for PEG-CNHs with an average size of 250 nm.[45] All samples showed good size dispersity with a polydispersity index (PDI) <0.2, see Table 1. Zeta potential measurements are a useful way to monitor surface transformations as well as the colloidal stability of nanoparticles.[46] The zeta potential of the CNHs at physiological pH (7.2) was found to be $\zeta = -49 \pm 7$ mV for **o-CNH** compared to +21 ± 3 mV for **CNH-HYZ** and −3 ± 5 mV for **CNH-PEG-NH₂** (Figure 2b, Table 1). These changes suggest that the ligands were successfully coupled onto the CNHs. The smaller change observed for the PEG functionalization may be due to steric hindrance caused by the long PEG chain which may have resulted is less functionalisation.

The non-covalent functionalised **o-CNH-PEI** hybrid systems (Family-2) were prepared by mixing suspensions of **o-CNH** (0.1-10 mg mL⁻¹) with concentrations of PEI (0.1-10 mg mL⁻¹) and

Table 1: Dynamic Light Scattering (DLS), Zeta Potential measurements and PDI of CNH suspensions post modifications

Carbon Nanohorn	o-CNH	CNH-HYZ	CNH-PEG-NH₂	o-CNH-PEI-A	o-CNH-PEI-B	o-CNH-PEI-C	o-CNH-PEI-D	o-CNH-PEI-E
CNHs (mg mL⁻¹)/PEI (mg mL⁻¹)	1:0	1:0	1:0	1:0.1	1:0.5	1:2.5	1:5	1:10
DLS (nm)	188 ± 80	219 ± 98	259 ± 107	232 ± 102	218 ± 106	252 ± 85	247 ± 72	261 ± 98
Zeta Potential (mV)	−49 ± 7	+ 21± 3	−3 ± 5	+ 23 ± 4	+ 34 ± 5	+ 42 ± 6	+ 47 ± 5	+ 54 ± 7
PDI	0.174	0.145	0.147	0.194	0.198	0.177	0.182	0.199

stirring overnight. Figure 3a shows the DLS and zeta potential results for the **o-CNH-PEI** hybrids **(A-E)** hybrids prepared using **o-CNH** (1 mg mL^{-1}) and PEI concentrations of **A** 0.1 mg mL^{-1}; **B** 0.5 mg mL^{-1}; **C** 2.5 mg mL^{-1}; **D** 5.0 mg mL^{-1} and **E** 10 mg mL^{-1}. The DLS data recorded for the samples showed an increase in the hydrodynamic diameter upon addition of the PEI, see Table 1. The presence of a single band together with the low PDI values (<0.2) indicated the absence of aggregation and the dispersion of discrete, coated CNH species. The presence of the PEI at the surface of the CNHs was confirmed by zeta potential measurements, which showed a dramatic shift in the zeta potential from –49 ± 7 mV (**o-CNH**) to +54 ± 6 mV (**o-CNH-PEI-E**; 1 mg mL^{-1}: 10 mg mL^{-1}), see Figure 3b. This shift in zeta potential is attributed to electrostatic interactions of the amine rich PEI to the negatively charged carboxylic acid moieties on the surface of the **o-CNH**. Similar trends were observed for hybrid systems developed using a lower CNH concentration (0.1 mg mL^{-1}), data not shown.

3.2 Preparation and Characterization of Family-1 CNH Biosensors incorporating o-CNH, CNH-PEG-NH$_2$ and CNH-HYZ

The influence of the covalently functionalised CNH modifiers on the biosensor performance was first investigated. To do this Family-1 biosensors were fabricated using low (0.1 mg mL^{-1}) and high (1 mg mL^{-1}) concentrations of **o-CNH**, **CNH-PEG-NH$_2$** and **CNH-HYZ**. The biosensors were prepared by 5 dip evaporations of the CNHs followed by 5 dip evaporations of the enzyme, and subsequent crosslinking with PEGDE which, can react with both amino and carboxyl groups. This yielded **Pt/o-CNH$_5$/GluOx$_5$**, **Pt/CNH-HYZ$_5$/GluOx$_5$**, and **Pt/CNH-PEG$_5$/GluOx$_5$** designs. SEM images recorded for **Pt/o-CNH$_5$**, and **Pt/CNH-PEG$_5$** showed immobilisation of the CNHs at the Pt surface. Non-uniform coverage on the biosensor

Fig. 3 (a) Dynamic light scattering (b) Zeta potential measurements of 1 mg mL^{-1} **o-CNH** and **o-CNH-PEI** hybrids (A-E), varying the concentration of PEI, obtained in ddH$_2$O, pH 7.2 at 25 °C.

surface with the two different CNH designs giving similar loading, see Fig. S2.

The performance of the CNH biosensors was assessed by analysing the parameters K_M, J_{MAX} and LRS (linear region slope), which are representative of enzyme biological activity, enzyme

Table 2: A comparison of the Biosensor parameters; J_{MAX}, K_M, and LRS for the designs Pt/GluOx$_5$, Pt/o-CNH$_5$/GluOx$_5$, Pt/(CNH-PEG-NH$_2$)$_5$/GluOx$_5$, and Pt/CNH-HYZ$_5$/GluOx$_5$ all prepares from a concentration of 0.1 mg mL^{-1}

Biosensor	J_{MAX} µA cm^{-2}	K_M mM	LRS µA cm^{-2} mM^{-1}
Pt/GluOx$_5$ (n = 6)	7 ± 2	0.26 ± 0.03	19 ± 5
Pt/o-CNH$_5$/GluOx$_5$ (n = 4)	18 ± 3	0.29 ± 0.05	35 ± 3
Pt/(CNH-PEG-NH$_2$)$_5$/GluOx$_5$ (n = 4)	20 ± 3	0.33 ± 0.09	39 ± 1
Pt/CNH-HYZ$_5$/GluOx$_5$ (n = 3)	15 ± 5	0.31 ± 0.11	26 ± 4

loading and biosensor sensitivity respectively. It is desirable to maintain the K_M low < 0.4 and as close in value to that observed of the unsupported GluOx, which has a K_M of 0.21 mM in solution.[42] The CNH biosensor results were compared to a control biosensor design which had no CNH present, *i.e.* GluOx deposited on the bare Pt surface (**Pt/GluOx$_5$**). Importantly, in all cases the presence of the CNH modifiers did not diminish the biological integrity of the GluOx enzyme, which is reflected in the low values of K_M (0.29 − 0.31 mM). The incorporation of **o-CNH** resulted in a significant increase in J_{MAX} from 7 ± 2 to 18 ± 3 µA cm^{-2} (p <0.007). This is quite interesting given the **o-CNH** negative surface charge (–49 ± 7 mV), which would not be expected to interact favourably with the anionic GluOx and its substrate glutamate. This suggests the possible increased loading of the GluOx due to interaction of the **o-CNH** sp^2 surface with hydrophobic and positively charged regions on the enzyme. It may also suggest a role of the PEGDE crosslinker. The greatest enhancement of GluOx loading was observed for the **CNH-PEG-NH$_2$** design J_{MAX} (20 ± 3 µA cm^{-2}, p<0.004), while a modest improvement was observed for the hydrazide system, see Table 2.

The presence of the CNHs was also found to increase the biosensor sensitivity with a similar trend in improvement observed. The presence of **o-CNH** in the design resulted in a significant increase in the LRS from 19 ± 5 µA cm^{-2} mM^{-1} to 35 ± 3 µA cm^{-2} mM^{-1} (p <0.05). The greatest improvement was observed for **CNH-PEG-NH$_2$** (p<0.002), which is attributed to the presence of the amine groups on the surface. Analysis of the performance revealed the **CNH-PEG-NH$_2$** and **o-CNH** biosensor designs to be statistically the similar with p-values of 0.74, 0.19 and 0.83 for the J_{MAX}, K_M and LRS, respectively. Interestingly, the inclusion of the more positively charged **CNH-HYZ** (ζ potential = +21 ± 3 mV) was not as effective as the other two systems. Taken together, these results suggest that the high surface area of the CNHs and the regions of sp^2 is the main contributing factor to the increased biosensor response.

Next the influence of the CNH modifier concentration on the biosensor performance was examined by increasing the CNH dipping solution from 0.1 mg mL^{-1} to 1 mg mL^{-1}. This increase in CNH concentration was not found to affect the biological integrity of the enzyme with no notable effect observed on the
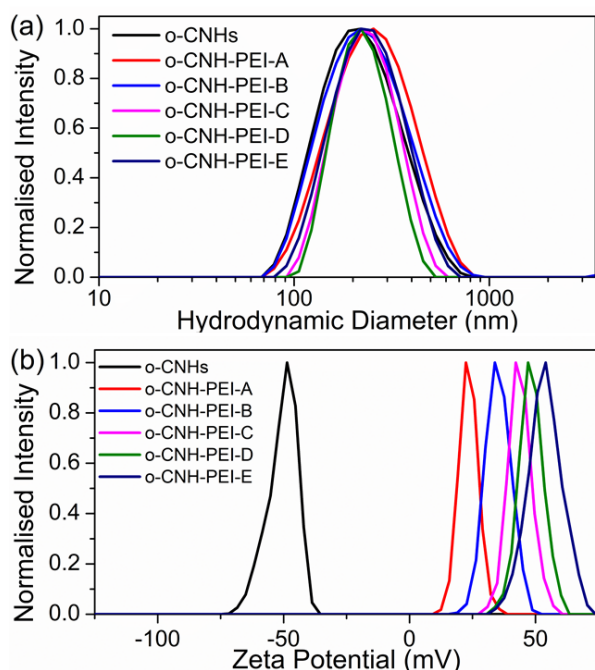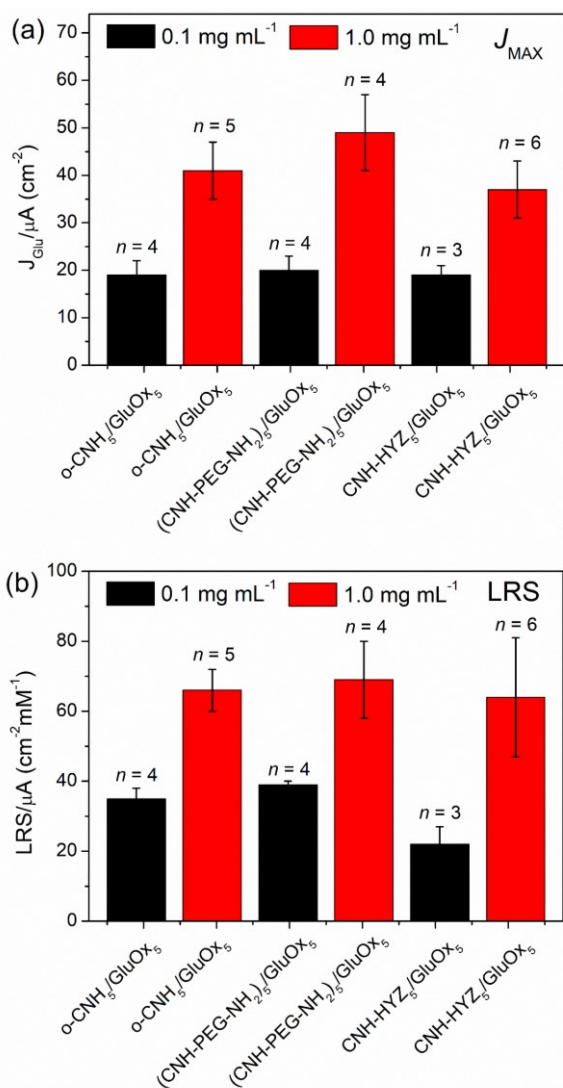
Fig. 4 Histograms showing a comparison between 3 different types of modified CNHs; o-CNH, CNH-PEG-NH$_2$ and CNH-HYZ as CNHs is increased from 0.1 mg mL^{-1} to 1 mg mL^{-1} corresponding to (a) the increase in the J_{MAX} and (b) the increase in the LRS.

K_M across all CNH designs at the two concentrations; at 0.1 mg mL^{-1} the K_M was 0.31 ± 0.04 mM, n = 11, and at 1 mg mL^{-1} the K_M was 0.34 ± 0.03 mM, n = 15 (p = 0.54). Critically, for the designs containing either **o-CNH**, **CNH- PEG-NH$_2$** or **CNH-HYZ**, an increase in the concentration from 0.1 mg mL^{-1} to 1 mg mL^{-1} resulted in an increase for both the J_{MAX} and the LRS of the biosensors in all cases (Figure 4). However, a further increase in concentration to 5 mg mL^{-1} led to CNH dispersion issues, resulting in an inhomogeneous, unstable semi suspension.

The value of the Hill coefficient, h, gives an indication of a deviation from Michaelis-Menton behaviour. When h = 1 there is thought to be neither cooperative nor non-cooperative binding between the substrate and the enzyme (or other modifiers present in the biosensor design). While, integral values of h > 1 are indicative of positive kinetic "cooperativity".[42,47] Non-integral h-values indicate non-specific binding of enzyme substrate somewhere in the calibration system. In the case of the basic design **Pt/GluOx$_5$** a h coefficient of close to unity was observed (1.04 ± 0.07, n = 6). At low concentration of the CNH modifier a similar value was obtained for **Pt/CNH-HYZ$_5$/GluOx$_5$** (0.9 ± 0.2 n = 3). However, the two highest performing designs, **Pt/o-CNH$_5$/GluOx$_5$** and **Pt/(CNH-PEG-NH$_2$)$_5$/GluOx$_5$**, were observed to have a higher h value of 1.29 ± 0.13 and 1.14 ± 0.05, respectively. Increasing the concentration of CNH modifier in these designs did not affect the h coefficient of the designs, see Table 3; there was no statistical difference between any of the designs where the modified concentration of CNH had been increased. These results suggest the possible role of non-specific or cooperative interactions in the increased performance. In addition, CNH-COOH have been shown to act as peroxidase enzyme mimics.[48] It is interesting to note that the least performing CNH modifier **(CNH-HYZ)** is the one for which the greatest number of COOH sites had been removed through functionalisation, as indicated by the zeta potential measurements. This indicates a possible role of the peroxidase activity in this system.

3.3 Preparation and characterisation of Family-2 CNH-PEI hybrid systems

Next the influence of non-covalently functionalised **o-CNH-PEI** modifiers on the biosensor performance was investigated. The Family-2 biosensors were fabricated in a similar way to Family-1, by 5 dip evaporations of the **o-CNH-PEI** followed by 5 dip evaporations of the enzyme, and subsequent crosslinking with PEGDE. Six **o-CNH-PEI** hybrid solutions, prepared from **o-CNH** (0.1 mg mL^{-1}, 1.0 mg mL^{-1}, 5.0 mg mL^{-1} and 10 mg mL^{-1}) and PEI (0.1 mg mL^{-1}, 5.0 mg mL^{-1} and 10 mg mL^{-1}) were examined. SEM images recorded for these electrodes indicated a significant increase amount of immobilisation of CNHs at the surface, see Fig. S3. This suggests a higher affinity for the hybrid systems for the Pt surface.

The performance of the biosensors was again tested by considering the K_M, J_{MAX} and LRS parameters. Importantly, the K_M remains at a desirable low value, an average value of 0.31 ± 0.01 mM, n = 28. The J_{MAX} and the LRS of the biosensor was found to be very sensitive to the composition of the **o-CNH-PEI** suspension, with the J_{MAX} displaying somewhat greater sensitivity, see Figure 5. Increasing the **o-CNH** concentration from 0.1 mg mL^{-1} to 1 mg mL^{-1} increased the biosensor response; yet, no further increase in sensitivity was obtained beyond 1 mg mL^{-1}, see Figure 5. An increase in concentration of the PEI was

Table 3: A comparison of the h coefficients for CNH Family-1 designs

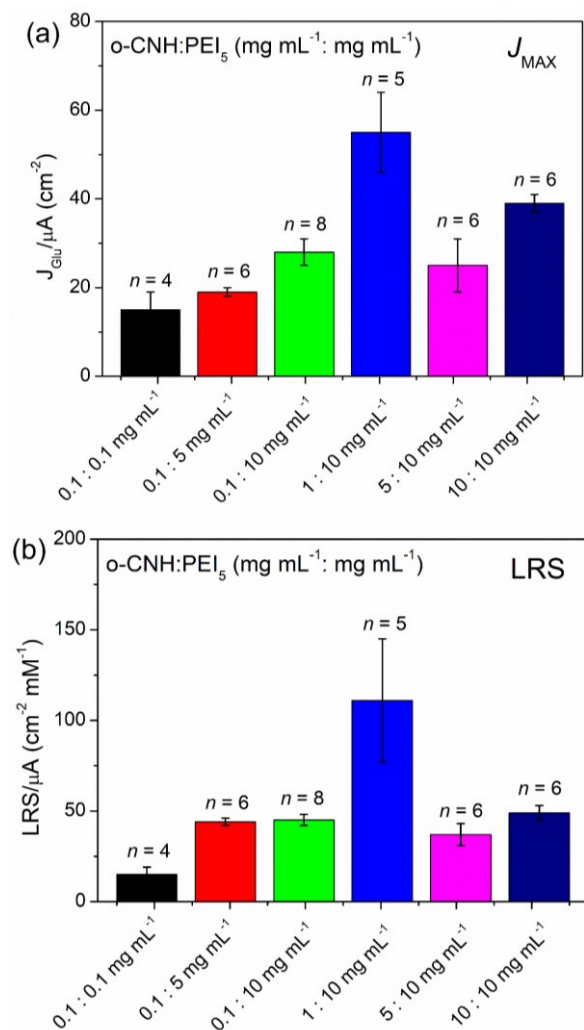| Biosensor	h coefficient (0.1 mg mL^{-1})	h coefficient (1.0 mg mL^{-1})	p-value
Pt/o-CNH$_5$/GluOx$_5$	1.29 ± 0.13 (n=4)	1.23 ± 0.02 (n = 5)	0.60
Pt/(CNH-PEG-NH$_2$)$_5$/GluOx$_5$	1.14 ± 0.05 (n = 4)	1.28 ± 0.13 (n = 4)	0.82
Pt/CNH-HYZ$_5$/GluOx$_5$	0.9 ± 0.2 (n = 3)	1.46 ± 0.13 (n = 5)	0.71

Fig. 5 Histograms depicting the increase in both the J_{MAX} and LRS of a **o-CNH-PEI** design as the concentration increases up to a maximum of 10 mg mL^{-1}:1 mg mL^{-1} **o-CNH-PEI**, after which, the J_{MAX} and LRS decline.

found to give the optimum in J_{max} and LRS up to a threshold of 10 mg mL^{-1} (which has been shown to be the optimum concentration previously[17]). The optimum design was identified to be **Pt/o-CNH-PEI$_5$/GluOx$_5$**, with **o-CNH-PEI** 10: 1 mg mL^{-1}. This design was found to be superior to (i) a PEI-free design **Pt/GluOx$_5$** and (ii) a PEI-containing (CNH-free) design, namely **Pt/PEI$_2$/GluOx$_5$**.[12] The average h coefficient for these designs was 1.49 ± 0.05, n = 32, when compared to a modifier-free design, Pt/GluOx$_5$ (h = 1.04 ± 0.07, n = 6), p < 0.004. This value again suggests a deviation from standard behaviour, which may indicate non-specific or cooperative interactions, or arise due to the presence of the **o-CNHs**. Overall the **o-CNH-PEI** was discovered to offer enhanced loading, in terms of J_{MAX} and LRS sensitivity, while maintaining a low K_M value. The best performing biosensor had a J_{max} of 55 ± 9 µA cm^{-2} and a LRS of 111 ± 34 µA cm^{-2} mM^{-1}, which is significantly improved on the previous best design, **Pt/PEI$_2$/GluOx$_5$** (J_{max} of 33 ± 1 µA cm^{-2} and a LRS of 42 ± 4 µA cm^{-2} mM^{-1}).

Table 4: The limit of detection, LOD and response times of biosensor designs of the form **Pt/CNH component/GluOx$_5$**.

CNH component	o-CNH/PEI$_5$ (mg mL^{-1})	LOD (µM)	Response times (s)
o-CNH$_5$ (n = 5)	1:0	0.45 ± 0.20	1.16 ± 0.26
CNH-HYZ$_5$ (n = 3)	1:0	0.06 ± 0.02	1.83 ± 0.44
CNH-PEG$_5$ (n = 4)	1:0	1.58 ± 0.34	0.95 ± 0.44
CNH-PEI$_5$ (n = 5)	1:10	0.02 ± 0.004	0.88 ± 0.13
CNH-PEI$_5$ (n = 4)	10:10	0.02 ± 0.007	1.15 ± 0.13

3.4 Comparison of Family-1 and Family-2

The presence of the **o-CNH-PEI** hybrid was found to significantly improve the biosensor performance. The influence of the hybrid can be seen by comparing the current observed with that of (i) the PEI free version (**CNH$_5$/GluOx$_5$**) and (ii) the previously best performing biosensor (**Pt/PEI$_2$/GluOx$_5$**), see Figure 6. An increase in current was observed for the CNH designs – **CNH-PEI** and **o-CNH** when compared to the non-CNH PEI design. This data clearly demonstrates the enhancement that is obtained in current when modified CNH are employed. Finally, the performance of the CNH biosensors was compared by considering the limit of detection (LOD) and the response times, which are important parameters for biosensor applications. Table 4 lists the LOD and response time of selected biosensors designed in this work. All the Biosensors displayed a fast response time (<2 s), making them suitable for future in-vivo work. The LOD values of these sensors were generally sub-micromolar, with the best designs exhibiting a LOD as low as 20 nM, again making them suitable for in-vivo use in brain ECF.
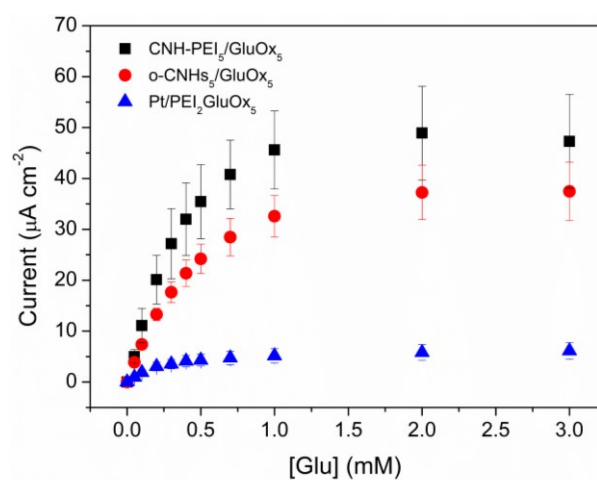

Fig. 6 The graph above shows 3 sets of data; **CNH-PEI$_5$/GluOx$_5$**, n = 5, **o-CNH$_5$/GluOx$_5$**, n = 5 and **Pt/PEI$_2$/GluOx$_5$** n = 6. Sets **CNH-PEI$_5$/GluOx$_5$** and **o-CNH$_5$/GluOx$_5$** have a p-value of 0.23, while **CNH-PEI$_5$/GluOx$_5$** and sets **Pt/PEI$_2$/GluOx$_5$** have a p-value of 0.0001.

Conclusions

Herein we report the use of discrete, modified carbon nanohorn dispersions to increase the sensitivity of a glutamate oxidase

biosensor. Numerous designs were generated using oxidized and covalently modified CNHs with a range of zeta potentials from −49 ± 7 mV to +21 ± 3 mV. Additionally, **CNH-PEI** hybrid formations were investigated by varying the concentration of CNHs and PEI to optimize the biosensor response. The surface charge of these nanoconstructs was dependent on the concentration of PEI added to the formulation, ranging from +54 ± 6 mV to +23 ± 4 mV. Notably, the hybrid systems showed no indication of significant aggregation and remained highly dispersed upon formation with a PDI < 0.2 for all systems.

SEM was used for visualization of these biosensor designs and confirmed the successful deposition of these CNH systems at the electrode surface. **o-CNH**, **CNH-HYZ** and **CNH-PEG-NH₂** (Family-1 designs) were introduced into biosensor designs and were successful in increasing both the J_{MAX} and LRS while maintaining a desirable low K_M value, which shows how the presence of the modified CNHs did not negatively affect the GluOx enzyme. Of the Family-1 CNHs investigated, it was determined that a concentration of 1 mg mL⁻¹ gave the best responses. **CNH-PEI** (Family-2 designs) was another system which was explored and gave an increased boost in biosensor parameters when compared to a CNH-free design and when compared Family-1 designs. The optimum **o-CNH:PEI** formulation was found to be 10: 1 mg mL⁻¹ and resulted in the most successful biosensor design reported here. This design is superior when compared to our previously partially optimized PEI-containing CNH-free design based on the recombinant form of GluOx used here.[17] The previous peroxidase-like activity of CNH-COOH[48] suggests a possible role in the systems reported here and presents the possibility to exploit this feature to improve sensitivity and detection limits.

Conflicts of interest

There are no conflicts to declare.

Acknowledgements

Notes and references

1   A. Lau and M. Tymianski, *Pflug Arch. Eur. J. Phy.*, 2010, **460**, 525–542.
2   S. Qin, M. Van Der Zeyden, W. H. Oldenziel, T. I. F. H. Cremers and B. H. C. Westerink, *Sensors*, 2008, **8**, 6860–6884.
3   G. Hughes, R. M. Pemberton, P. R. Fielden and J. P. Hart, *TrAC, Trends Anal. Chem.*, 2016, **79**, 106–113.
4   P. Nandi and S. M. Lunte, *Anal. Chim. Acta*, 2009, **651**, 1–14.
5   V. I. Chefer, A. C. Thompson, A. Zapata and T. S. Shippenberg, *Curr. Protoc. Neurosci.*, 2009, **7**,1–28.
6   K. L. Clapp-Lilly, R. C. Roberts, L. K. Duffy, K. P. Irons, Y. Hu and K. L. Drew, *J. Neurosci. Methods*, 1999, **90**, 129–142.
7   S. K. Hamdan and Z. M. Zain, *Malays. J. Med. Sci.*, 2014, **21**, 11–25.
8   S. Govindarajan, C. J. McNeil, J. P. Lowry, C. P. McMahon and R. D. O'Neill, *Sens Actuators B Chem.*, 2013, **178**, 606–614.
9   J. Wang, *J. Pharm. Biomed. Anal.*, 1999, **19**, 47–53.
10 M. Miele and M. Fillenz, *J. Neurosci. Methods*, 1996, **70,** 15–19.
11 S. M. Kirwan, G. Rocchitta, C. P. McMahon, J. D. Craig, S. J. Killoran, K. B. O'Brien, P. a. Serra, J. P. Lowry and R. D. O'Neill, *Sensors*, 2007, **7**, 420–437.
12 R. Ford, S. J. Quinn and R. D. O'Neill, *Sensors*, 2016, **16**, 11–13.
13 N. Vasylieva, B. Barnych, A. Meiller, C. Maucler, L. Pollegioni, J.S. Lin, D. Barbier and S. Marinesco, *Biosens. Bioelectron*. 2011, **26**, 3993–4000.
14 N. Vasylieva, C. Maucler, A. Meiller, H. Viscogliosi, T. Lieutaud, D. Barbier and S. Marinesco, *Anal. Chem.*, 2016, **85**, 2507–2515.
15 S. A Bhakta, E. Evans, T.E. Benavidez and C.D. Garcia, *Anal. Chim. Acta.*, 2015, **872**, 7–25.
16 M. Hersey, S. Berger, J. Holmes, A. West and P. Hashemi, *Anal. Chem.* 2019, **91**, 27–43
17 F. R. Baptista, S. A. Belhout , S. Giordani and S. J. Quinn, *Chem. Soc. Rev.*, 2015, **44**, 4433-4453
18 Y. Shao, J. Wang, H. Wu, J. Liu, I. A. Aksay and Y. Lina, *Electroanalysis*, 2010, **22**, 1027–1036
19 T.A. Silva, F.C. Moraes, B.C. Janegitz, O. Fatibello-Filho and R.W. Lu, *J. Nanomater.* 2017, 4571614, 14.
20 C. Zanardi, E. Ferrari, L. Pigani, F. Arduini and R. Seeber, *Chemosensors*, 2015, **3**, 118–128.
21 F. Arduini, M. Forchielli, A. Amine, I. Neagu, I. Cacciotti, F. Nanni, D. Moscone and G. Palleschi, *Microchim. Acta*, 2014, **182**, 643–651.
22 S. Sotiropoulou and N.A. Chaniotakis, *Anal. Bioanal. Chem.*, 2003, **375**, 103-105.
23 R. Khan, W. Gorski and C.D. Garcia, *Electroanalysis*, 2011, **23** 2357-2363.
24 N. Isoaho, E. Peltola, S. Sainio, N. Wester, V. Protopopova, J. Koskinen and T. Laurila, *J. Phys. Chem. C*, 2017, **121**, 4618–4626
25 V. Vamvakaki, K. Tsagaraki and N. Chaniotakis, *Anal. Chem.*, 2006, **78**, 5538–5542
26 C. Shan, H. Yang, J. Song, D. Han, A. Ivaska and L. Niu. *Anal. Chem.*, 2009, **81**, 2378–2382
27 J. Hu, S. Wisetsuwannaphum and J.S. Foord, *Faraday Discuss.* 2014, **172**, 457-72
28 X. Kang, J. Wang, H. Wu, I. A. Aksay, J. Liu and Y. Lin, *Biosens. Bioelectron.*, 2009, **25**, 901–905.
29 M. Pumera, A. Ambrosi, A. Bonanni, E. L. K. Chng and H. L. Poh, *Trends Anal. Chem.,* 2010, **29**, 954–965.
30 S.Iijima, M.Yudasaka, R.Yamada, S.Bandow, K.Suenaga, F.Kokai and K.Takahashi, *Chem. Phys. Lett.*, 1999, **309**, 165−170
31 H. Isobe, T. Tanaka, R. Maeda, E. Noiri, N. Solin, M. Yudasaka, S. Iijima and E. Nakamura, *Angew. Chem. Int. Ed.*, 2006, **45**, 6676–6680.
32 J. Miyawaki, M. Yudasaka, T. Azami, Y. Kubo and S. Iijima, *ACS Nano*, 2008, **2**, 213–226.
33 N. Karousis, I. Suarez-Martinez, C. P. Ewels and N. Tagmatarchis, *Chem. Rev.*, 2016, **116**, 4850–4883.
34 D. Kase, J. L. Kulp, M. Yudasaka, J. S. Evans, S. Iijima and K. Shiba, *Langmuir*, 2004, **20**, 8939–8941.
35 X. Liu, L. Shi, W. Niu, H. Li and G. Xu, *Biosens. Bioelectron.*, 2008, **23**, 1887–1890.
36 X. Liu, H. Li, F. Wang, S. Zhu, Y. Wang and G. Xu, *Biosens. Bioelectron.*, 2010, **25**, 2194–2199.
37 S. Zhu, X. Zhao, J. You, G. Xu, H. Wang, Analyst, 2015, **140**, 6398.
38 B. Lu, Z. Zhang, J. Hao, G. Xu, B. Zhang and J. Tang, *Anal. Methods*, 2012, **4**, 3580-3585.

39 S. J. Devereux, S. Cheung, H. C. Daly, D. F. O'Shea and S J. Quinn, *Chem. Eur. J*., 2018, **24,** 14162-14170.

40 M. Schiavon, Europe patent EP1428794 (A2); 2004 June 16.

41 M. Schiavon, .US2004213727 (A1); 2004 October 28.

42 B.I. Kurganov, A.V. Lobanov, I.A. Borisov and A.N. Reshetilov, *Anal. Chim. Acta.*, 2011, **427**, 11–19.

43 C. Y. Shu, J. Zhang, J. C. Ge, J. H. Sim, B. G. Burke, K. A. Williams, N. M. Rylander, T. Campbell,   A. Puretzky, C. Rouleau, D. B. Geohegan, K. More, A. R. Esker, H. W. Gibson and H. C. Dorn, *Chem. Mater.* 2010, **22**, 347–351.

44 E. Miyako, H. Nagata, K. Hirano, K. Sakamoto, Y. Makita, K. Nakayama and T. Hirotsu, *Nanotechnology*, 2008, **19**, 075106-07511.

45 T. Murakami, J. Fan, M. Yudasaka, S. Iijima and K. Shiba, *Mol. Pharmaceutics*, 2006, **3**, 407-414.

46 F. Thielbeer, K. Donaldson and M. Bradley, *Bioconjugate Chem.*, 2011, **22**, 144–150.

47 E. V. Emelyanova, *Journal of Biotechnology and Biomedical Science*, 2018, **3**, 94-99.

48 S. Zhu, X. En Zhao, J. You, G. Xu and H. Wang, *Analyst*, 2015, **140**, 6398-6403.